

Mesa-Sidewall Effect on Coherent Terahertz Radiation via Spontaneous Synchronization of Intrinsic Josephson Junctions in $\text{Bi}_2\text{Sr}_2\text{CaCu}_2\text{O}_{8+\delta}$

G. Kuwano,¹ M. Tsujimoto^{1,2,*}, Y. Kaneko,¹ T. Imai,¹ Y. Ono,¹ S. Nakagawa,¹ S. Kusunose,¹ H. Minami,^{1,2} T. Kashiwagi,^{1,2} K. Kadowaki,³ Y. Simsek,^{4,5} U. Welp,⁴ and W.-K. Kwok⁴

¹Graduate School of Pure and Applied Sciences, University of Tsukuba, 1-1-1 Tennodai, Tsukuba, Ibaraki, 305-8573, Japan

²Faculty of Pure and Applied Sciences, University of Tsukuba, 1-1-1 Tennodai, Tsukuba, Ibaraki, 305-8573, Japan

³Algae Biomass and Energy System R&D Center, University of Tsukuba, 1-1-1 Tennodai, Tsukuba, Ibaraki, 305-8572, Japan

⁴Materials Science Division, Argonne National Laboratory, Lemont, Illinois 60439, USA

⁵Sabancı University Nanotechnology Research and Application Center, Tuzla, Istanbul 34956, Turkey



(Received 13 August 2019; revised manuscript received 4 November 2019; published 21 January 2020)

We investigate the effect of the $\text{Bi}_2\text{Sr}_2\text{CaCu}_2\text{O}_{8+\delta}$ mesa sidewall on the spontaneous synchronization of intrinsic Josephson junctions and concomitant terahertz radiation. We develop a lithography technique to control the sidewall angles. Using a Fourier interferometer, we characterize the radiation emitted from a series of mesas with different sidewall angles. We determine that a uniform distribution of the oscillation frequencies is essential to produce coherent radiation outside the mesa. It is also noted that in the resonant state, the input excess energy is transferred to the excitation of the coherent state.

DOI: [10.1103/PhysRevApplied.13.014035](https://doi.org/10.1103/PhysRevApplied.13.014035)

I. INTRODUCTION

The realization of compact, solid-state, and coherent terahertz (1 THz = 10^{12} Hz) sources has received extensive attention in different fields of science and in industry [1], with potential applications to sensing [2], imaging [3], and spectroscopy [4]. Remarkable progress has been achieved in the development of terahertz sources based on semiconductor devices [5]: Gunn, impact-injection avalanche transit-time (IMPATT), and tunnel-injection transit-time (TUNNETT) diodes can generate intense radiation below 0.3 THz, while quantum-cascade lasers can emit powerful radiation at frequencies greater than 1.45 THz, although they must be cooled to 37 K [6]. A resonant tunneling diode [7] can generate frequencies approaching 1.92 THz, even at room temperature [8]; however, an emission power greater than 1 mW remains unattainable.

Coherent and tunable terahertz radiation from atomic-scale stacks of intrinsic Josephson junctions (IJJs) [9] in anisotropic cuprate high- T_c superconductors has provided a promising usable technology in the terahertz regime [10]. See Refs. [11–13] for recent reviews. The application of a dc voltage V to a mesa structure made of single-crystal $\text{Bi}_2\text{Sr}_2\text{CaCu}_2\text{O}_{8+\delta}$ (Bi-2212) has enabled electromagnetic generation at the Josephson frequency, $f_J = (2e/h) \times V/N$, where N is the number of stacked IJJs and

e and h are the elementary charge and Planck's constant, respectively [14]. A maximum output power of 0.6 mW at 0.5 THz was obtained from arrayed mesas [15], which is currently the highest recorded level among all solid-state terahertz sources. The spectral linewidth down to approximately 20 MHz was measured with a superconducting integrated receiver [16]. One of the potential advantages of Bi-2212 sources compared with the aforementioned semiconducting approaches is their broad tunability. The frequency can be tuned either by changing the bath temperature [17,18] or by examining the internal current-voltage branches [19], where the reported broadest band extends continuously from 0.5 to 2.4 THz [20].

In a pioneering study, Wiesenfeld *et al.* [21,22] obtained a complete phase-locked synchronization in a disordered Josephson-junction array. Here, within limits of weak coupling and disorder, the overdamped junction array, which is shunted by an inductor-capacitor-resistor load, can be mapped onto an exactly solvable Kuramoto model [23], which is a mathematical model used to describe synchronization of a large set of coupled oscillators. Nonlinearly coupled IJJs can also synchronize to a common frequency determined by their geometries [10,24–28]. Such a remarkable synchronization phenomenon has been observed in numerous physical and biological systems, including relaxation oscillator circuits, networks of neurons, cardiac pacemaker cells, and fireflies that flash in union [29].

*tsujimoto@ims.tsukuba.ac.jp

Some previous studies show that a tilted mesa sidewall due to the trapezoidal cross-section shape produces a distribution of junction properties [18,30,31], such as quasiparticle resistance, Josephson current, and intrinsic capacitance. These distributions are expected to cause the nontrivial gradient of the junction voltage and oscillation frequency along the stack. In general, controlling the sidewalls of light-emitting devices has been demonstrated to improve the overall characteristics. For example, the reduction of sidewall roughness can lead to scattering losses on a silicon-on-insulator waveguide [32]. In the case of gallium nitride diode lasers, the tilted sidewalls can cause the deflection of photons guided within an epilayer, resulting in low emission efficiencies [33].

In this work, we demonstrate that uniform stacks can provide physical realizations of the efficient synchronization of stacked IJJs. To investigate the effect of characteristic distribution, we develop a fabrication technique based on UV lithography to control the sidewall angle. We observe that as the distribution increases, the system fails to remain in a coherent state, resulting in the loss of radiation output.

II. EXPERIMENT

A Bi-2212 single crystal is grown by the traveling-solvent floating-zone method. A piece of the crystal is annealed at 600 °C for 24 h in argon gas mixed with 0.1% oxygen. The crystal is glued onto a sapphire substrate with use of heat-conductive silver paste. The crystal is cleaved under a microscope and a 30-nm silver layer is immediately evaporated onto the surface. To pattern two Bi-2212 mesas with different sidewall angles, we use two types of photoresists in a UV-lithography process: a chemically amplified photoresist (TCIR series, Tokyo Ohka Kogyo Co. Ltd.) and a novolac photoresist (OFPR series, Tokyo Ohka Kogyo Co. Ltd.). The process for controlling the sidewall angle relies on the cross-section profile and dry-etch resistance. The two mesas are milled from the same crystal base by an argon-ion-milling technique. Then a 140-nm silver layer is evaporated over the top surface and etched with a lithography technique to pattern the top electrode. Figure 1(a) depicts the SEM image of two neighboring mesas; namely, mesa A and mesa B. Two strip silver electrodes are highlighted in blue and blacked out over the insulating resin layer in Fig. 1(a). The gray-rimmed edges of the two mesas differ significantly in thickness and contrast, indicating different sidewall angles for each mesa. Figure 1(b) displays the cross-section profiles measured by atomic force microscopy. The electrode layer atop the mesa is indicated by blue shading. The actual sizes of the two mesas are summarized in Table I. The identical thickness t of 1 μm corresponds to 667 IJJs for each mesa. The variation in the sidewalls can be explained by the shapes and etch resistances of the photoresist layers, the different

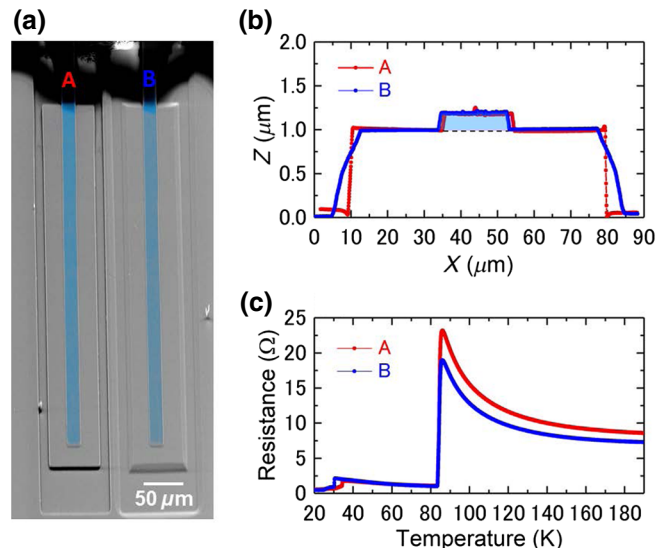


FIG. 1. (a) SEM image of two mesas fabricated on an identical Bi-2212 crystal base. (b) Cross-section profiles for mesas A and B measured by atomic force microscopy. (c) Temperature dependence of c -axis resistance.

development rate, and dark erosion issue in a developer. We also note that the etch resistance depends strongly on the thermal condition during ion milling. Here we define the degree of distortion as follows:

$$\gamma = \frac{1-r}{1+r}, \quad (1)$$

where $r = w_t/w_b$ is determined by the top and bottom widths, and γ corresponds to the distribution width of the junction characteristics of the system. From the actual data displayed in Fig. 1(b), we calculate γ of 1.6% for mesa A and 10.8% for mesa B (see Table I). Note that γ less than 2% was not achieved in most previous studies.

Figure 1(c) displays the temperature dependence of the c -axis resistances for mesa A (red) and mesa B (blue). The onset superconducting critical temperature T_c of 87.0 K is the same for the two mesas. This demonstrates the uniformity of the superconducting properties in the bulk crystal. The additional transition visible near 30 K is likely attributable to the damaged surface layer [34].

The sample is mounted on a cold finger of a Gifford-McMahon cryocooler. We use a silicon hemispherical lens of radius 3.1 mm to collimate the emitted terahertz waves.

TABLE I. Profile parameters of Bi-2212 mesas.

Parameter	Mesa A	Mesa B
w_t (μm)	68.7	64.6
w_b (μm)	71.0	80.3
t (μm)	0.99	0.98
γ (%)	1.6	10.8

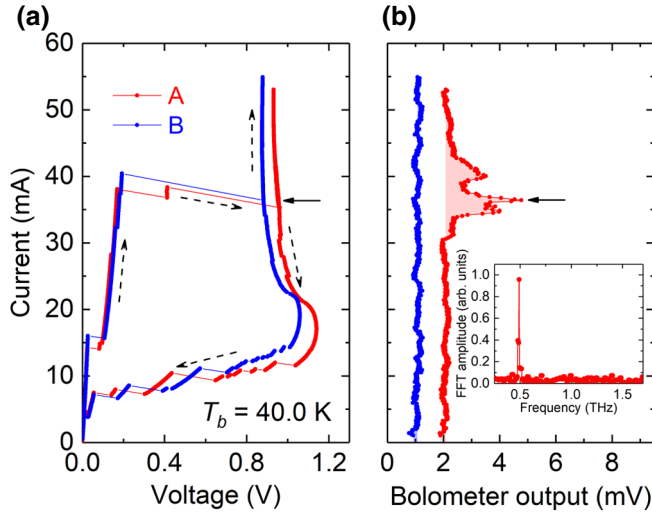


FIG. 2. (a) Current-voltage characteristics and (b) lock-in signals from a silicon-composite bolometer at $T_b = 40.0$ K. Dashed arrows indicate the current-sweep direction. The inset shows the Fourier-transform spectrum measured at the highest peaks of the bolometer output, indicated by arrows in (a),(b).

Meanwhile, the mesas are biased with use of a function generator, and the current-voltage characteristics (IVCs) are monitored with conventional electronic devices. Additionally, we use a silicon-composite bolometer to detect the radiation. A Fourier-transform interferometer system of our own design based on a split mirror [35] is used to measure the radiation frequencies. The scanning length of 35 mm corresponds to a frequency resolution of 4 GHz.

III. RESULTS AND DISCUSSION

Figure 2(a) displays the IVCs for mesa A (red) and mesa B (blue) measured at a bath temperature T_b of 40.0 K. The IVC curves indicate large hysteresis between increasing-bias-current and decreasing-bias-current branches typical of an underdamped IJJ array. The system switches from the zero-voltage state to the resistive state at 40 mA. The observed back-bending behavior in the IVCs can be attributed to the self-heating effect. The data displayed in Fig. 2(b) represent the bolometer output signals obtained with the lock-in technique.

The bolometer outputs clearly indicate that mesa A emits radiation in the high-bias regime in a relatively wide range of bias currents from 33.7 to 42.7 mA. The inset in Fig. 2(b) displays the Fourier-transform spectrum measured at the highest peak of the bolometer signal [see arrows in Figs. 2(a) and 2(b)]. The radiation frequency f of 0.499 THz is obtained at this particular bias point. By our sweeping bias points, f is weakly tunable according to the ac Josephson relation. Meanwhile, the output intensity reaches a maximum at the rectangular cavity frequency f_{10}^r with a refractive index n of 4.2 [10,24]. Conversely,

no apparent radiation is observed on mesa B at the overall bath temperature. This strongly indicates that complete synchronization is not achieved among the stacked IJJs owing to the tilted sidewalls of mesa B. Note that the damaged surface layers are not likely to contribute directly to radiation because T_b and the actual local temperature of the emitting mesa exceed 30.0 K [see Fig. 1(c)].

Another interesting observation relates to the thermal properties of Bi-2212 mesas. Extensive investigations in the literature have shown that biased mesas are susceptible to nonuniform temperature distributions accompanied by sizable temperature gradients in the a - b plane as well as along the c axis direction [16,17,36–52]. The effect of such temperature inhomogeneities on the electromagnetic properties is still under investigation. Previous experimental work demonstrated that high-bias emission occurs at a significantly lower frequency than expected from the Josephson relation [42]. This behavior is consistent with our results and is attributed to the strongly nonuniform self-heating effect. The thermal simulation also reveals that the junction voltage can be distributed along the c axis owing to low thermal conductivity and large temperature coefficients of the c -axis quasiparticle resistances [38,43].

It is also worth noting that we tested other identical mesas with different sidewall angles to validate the repeatability of the sidewall effect. The experimental data obtained are summarized in Supplemental Material [53]. From such repeated measurements, we conclude that the absence of emission is primarily not caused by the self-heating effect but is most likely due to the suppression of synchronization brought about by the trapezoidal cross section. The observed transition is qualitatively consistent with the Kuramoto model, where increase in the distribution of oscillation frequencies leads to synchronization failure. To determine the threshold value of γ required for synchronization, we need more data points at $\gamma < 10.8\%$.

To examine the coherent behavior of the system with respect to variations in thermal conditions, we plot the IVCs as a function of T_b with color-coded bolometer outputs in Fig. 3. T_b was stabilized in the range from 20.0 to 50.0 K in steps of 5 K with use of proportional-integral-differential control. As T_b increases, the IVC hysteresis is suppressed significantly owing to the reduction of c -axis quasiparticle resistance. As can be observed in the color-coded power map in Fig. 3, intense radiation is seen when f_J approximately matches f_{10}^r in the high-bias regime. In the low-bias regime below 10 mA, no radiation is observed, possibly because f_J cannot satisfy the cavity conditions owing to retrapping as evidenced by the series of steps in the IVC curve [Fig. 2(a)] occurring for decreasing bias current.

The observed f is weakly tunable by approximately 10% in the overall T_b range. In the most previous studies, large frequency tunability Δf of 40%–50% or more arose when T_b was scanned [17,18,20,27,28,46,54–56].

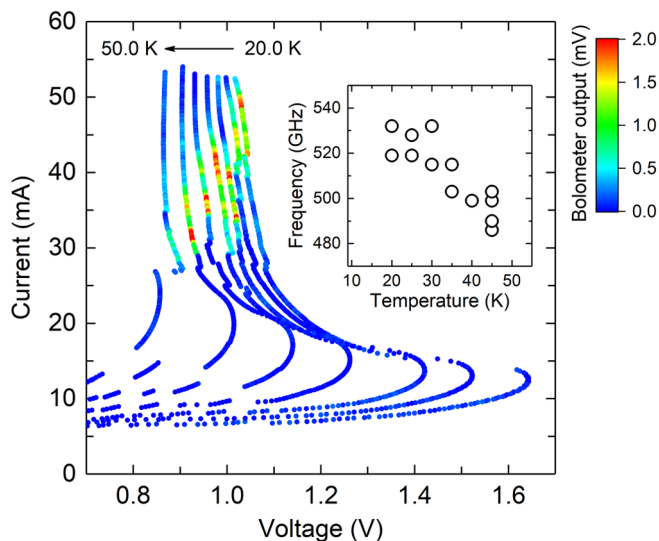


FIG. 3. T_b dependence of IVCs with color-coded bolometer output for mesa A. T_b is stabilized in the range from 20.0 to 50.0 K in steps of 5.0 K. The inset should f tunability versus T_b .

The tunability was assumed to be due to the temperature dependence of the London penetration depth [18]. In the inset in Fig. 3, we plot the variation of the emission frequency as a function of T_b . Because the quality factor of the resonance is inversely proportional to Δf in general, we assume that the quality factor of mesa A is virtually half that of the previous samples. Although the connection may not be straightforward, the quality of resonance could be increased when γ is less than 1.6%. In this sense, it seems that mesas with lower γ show narrow tunability in comparison with the usual mesas. Further quantitative measurements of the spectral linewidths using a heterodyne technique [57] could reveal the relationship between the mesa sidewall and quality of the resonance more clearly.

In the resonant state, an excess current is injected into the IJJ system that drives the cavity excitation [10,18]. A small fraction of the associated input power is converted to outside radiation. Figures 4(a) and 4(b) display enlarged views of the return IVC branches and detected radiation power on a color-coded scale for mesa A and mesa B, respectively. The absence of jumps in the IVCs allows us to roughly estimate the baselines of the current (see the dashed lines) and to determine the amounts of excess current. These data suggest that 2–3 mW, which is approximately 10% of the input power calculated from the product of voltage and current, is pumped into the system, implying that considerably enhanced radiation could be observed from both mesas. Nevertheless, the integrated radiation power is significantly smaller or even negligible for mesa B, where the oscillation frequencies are distributed along the stack owing to its trapezoidal profile. We assume that for mesa B the excess energy is consumed to excite the

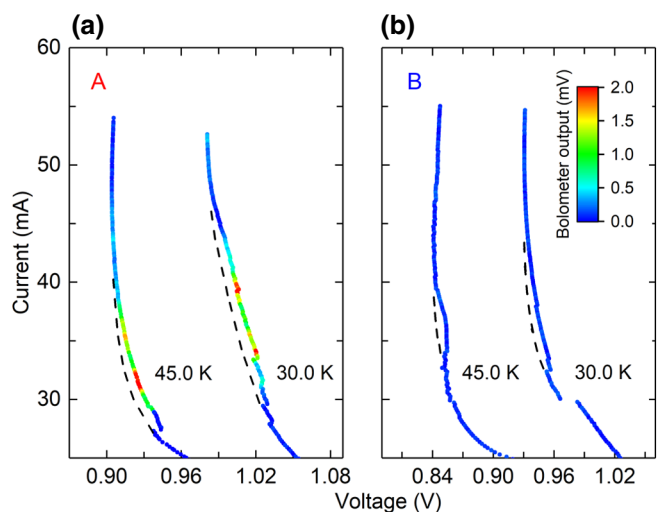


FIG. 4. Magnified views of returning IVC branches and detected radiation power on a color-coded scale for (a) mesa A and (b) mesa B. Dashed lines represent baselines of IVCs with the assumption that input excess energy is transferred to excitation of the resonant state.

incoherent state. A possible dynamic state of a nonlinearly coupled IJJ system was theoretically predicted in previous studies using a computational approach [18,58–62]. For the coherent state, the electric fields from the junctions are added to create an intense wave and radiation. In contrast, in the incoherent state, the electric fields are largely canceled, resulting in negligible radiation. Because the super-radiant power is proportional to the square of the number of IJJs in the coherent state [10], a group of excited standing waves in mesa B could be canceled in the far-field detection despite the enormous amount of input power, even when $f_J = f_{10}^r$.

IV. CONCLUSION

In summary, we investigate the effects of the out-of-plane characteristic distribution of IJJs stacked in a Bi-2212 mesa on spontaneous synchronization for coherent terahertz radiation. We develop a lithography technique to control the mesa sidewall angles. Using a Fourier interferometer, we characterize the radiation properties of on-chip mesas with different sidewall angles. We determine that the uniform distribution of the oscillation frequencies, observed in mesas with lower γ , is important and essential to produce coherent radiation outside the mesas. This result is qualitatively consistent with the Kuramoto model for a large number of nonlinearly coupled Josephson junctions. The input excess energy quantified in the bumps of the IVCs is transferred to the excitation of the resonant state. Most importantly, the coherent and incoherent states are experimentally identified. These findings allow us to construct highly efficient superconducting sources of intense

and tunable terahertz radiation that allow better technology development for this frequency regime.

ACKNOWLEDGMENTS

The authors thank T. Yamamoto for providing single crystals of Bi-2212. This work was supported by the Japan Society for the Promotion of Science (JSPS) KAKENHI (Grant No. 19H02540) and JSPS Overseas Research Fellowships, the Program to Disseminate the Tenure Tracking System at the University of Tsukuba, and the U.S. Department of Energy, Office of Science, Basic Energy Sciences, Materials Sciences and Engineering Division.

-
- [1] M. Tonouchi, Cutting-edge terahertz technology, *Nat. Photonics* **1**, 97 (2007).
- [2] D. Mittleman, *Sensing with Terahertz Radiation*, edited by D. Mittleman, Springer Series in Optical Sciences, Vol. 85 (Springer Berlin Heidelberg, Berlin, Heidelberg, 2003).
- [3] D. M. Mittleman, M. Gupta, R. Neelamani, R. G. Baraniuk, J. V. Rudd, and M. Koch, Recent advances in terahertz imaging, *Appl. Phys. B: Lasers Opt.* **68**, 1085 (1999).
- [4] P. Jepsen, D. Cooke, and M. Koch, Terahertz spectroscopy and imaging – Modern techniques and applications, *Laser Photon. Rev.* **5**, 124 (2011).
- [5] S. S. Dhillon *et al.*, The 2017 terahertz science and technology roadmap, *J. Phys. D: Appl. Phys.* **50**, 043001 (2017).
- [6] S. Kumar, Recent progress in terahertz quantum cascade lasers, *IEEE J. Sel. Top. Quantum Electron.* **17**, 38 (2011).
- [7] E. R. Brown, J. R. Söderström, C. D. Parker, L. J. Mahoney, K. M. Molvar, and T. C. McGill, Oscillations up to 712 GHz in InAs/AlSb resonant-tunneling diodes, *Appl. Phys. Lett.* **58**, 2291 (1991).
- [8] T. Maekawa, H. Kanaya, S. Suzuki, and M. Asada, Oscillation up to 1.92 THz in resonant tunneling diode by reduced conduction loss, *Appl. Phys. Express* **9**, 024101 (2016).
- [9] R. Kleiner, F. Steinmeyer, G. Kunkel, and P. Müller, Intrinsic Josephson Effects in Bi₂Sr₂CaCu₂O₈ Single Crystals, *Phys. Rev. Lett.* **68**, 2394 (1992).
- [10] L. Ozyuzer, A. E. Koshelev, C. Kurter, N. Gopalsami, Q. Li, M. Tachiki, K. Kadowaki, T. Yamamoto, H. Minami, H. Yamaguchi, T. Tachiki, K. E. Gray, W.-K. Kwok, and U. Welp, Emission of coherent THz radiation from superconductors, *Science* **318**, 1291 (2007).
- [11] U. Welp, K. Kadowaki, and R. Kleiner, Superconducting emitters of THz radiation, *Nat. Photonics* **7**, 702 (2013).
- [12] I. Kakeya and H. Wang, Terahertz-wave emission from Bi-2212 intrinsic Josephson junctions: A review on recent progress, *Supercond. Sci. Technol.* **29**, 073001 (2016).
- [13] T. Kashiwagi, H. Kubo, K. Sakamoto, T. Yuasa, Y. Tanabe, C. Watanabe, T. Tanaka, Y. Komori, R. Ota, G. Kuwano, K. Nakamura, T. Katsuragawa, M. Tsujimoto, T. Yamamoto, R. Yoshizaki, H. Minami, K. Kadowaki, and R. A. Klemm, The present status of high- T_c superconducting terahertz emitters, *Supercond. Sci. Technol.* **30**, 074008 (2017).
- [14] B. Josephson, Possible new effects in superconductive tunnelling, *Phys. Lett.* **1**, 251 (1962).
- [15] T. M. Benseman, K. E. Gray, A. E. Koshelev, W.-K. Kwok, U. Welp, H. Minami, K. Kadowaki, and T. Yamamoto, Powerful terahertz emission from Bi₂Sr₂CaCu₂O_{8+ δ} mesa arrays, *Appl. Phys. Lett.* **103**, 022602 (2013).
- [16] M. Li, J. Yuan, N. Kinev, J. Li, B. Gross, S. Guénon, A. Ishii, K. Hirata, T. Hatano, D. Koelle, R. Kleiner, V. P. Koshelevs, H. Wang, and P. Wu, Linewidth dependence of coherent terahertz emission from Bi₂Sr₂CaCu₂O₈ intrinsic Josephson junction stacks in the hot-spot regime, *Phys. Rev. B* **86**, 060505 (2012).
- [17] H. B. Wang, S. Guénon, B. Gross, J. Yuan, Z. G. Jiang, Y. Y. Zhong, M. Grünzweig, A. Iishi, P. H. Wu, T. Hatano, D. Koelle, and R. Kleiner, Coherent Terahertz Emission of Intrinsic Josephson Junction Stacks in the Hot Spot Regime, *Phys. Rev. Lett.* **105**, 057002 (2010).
- [18] T. M. Benseman, A. E. Koshelev, K. E. Gray, W. Kwok, U. Welp, K. Kadowaki, M. Tachiki, and T. Yamamoto, Tunable terahertz emission from Bi₂Sr₂CaCu₂O_{8+ δ} mesa devices, *Phys. Rev. B* **84**, 064523 (2011).
- [19] M. Tsujimoto, T. Yamamoto, K. Delfanazari, R. Nakayama, T. Kitamura, M. Sawamura, T. Kashiwagi, H. Minami, M. Tachiki, K. Kadowaki, and R. A. Klemm, Broadly Tunable Sub-terahertz Emission from Internal Current-Voltage Characteristic Branches Generated from Bi₂Sr₂CaCu₂O_{8+ δ} , *Phys. Rev. Lett.* **108**, 107006 (2012).
- [20] T. Kashiwagi, K. Sakamoto, H. Kubo, Y. Shibano, T. Enomoto, T. Kitamura, K. Asanuma, T. Yasui, C. Watanabe, K. Nakade, Y. Saiwai, T. Katsuragawa, M. Tsujimoto, R. Yoshizaki, T. Yamamoto, H. Minami, R. A. Klemm, and K. Kadowaki, A high- T_c intrinsic Josephson junction emitter tunable from 0.5 to 2.4 terahertz, *Appl. Phys. Lett.* **107**, 082601 (2015).
- [21] K. Wiesenfeld, P. Colet, and S. Strogatz, Synchronization Transitions in a Disordered Josephson Series Array, *Phys. Rev. Lett.* **76**, 404 (1996).
- [22] K. Wiesenfeld, P. Colet, and S. Strogatz, Frequency locking in Josephson arrays: Connection with the Kuramoto model, *Phys. Rev. E* **57**, 1563 (1998).
- [23] Y. Kuramoto, *Chemical Oscillations, Waves, and Turbulence*, Springer Series in Synergetics, Vol. 19 (Springer Berlin Heidelberg, Berlin, Heidelberg, 1984).
- [24] M. Tsujimoto, K. Yamaki, K. Deguchi, T. Yamamoto, T. Kashiwagi, H. Minami, M. Tachiki, K. Kadowaki, and R. A. Klemm, Geometrical Resonance Conditions for THz Radiation from the Intrinsic Josephson Junctions in Bi₂Sr₂CaCu₂O_{8+ δ} , *Phys. Rev. Lett.* **105**, 037005 (2010).
- [25] T. Kashiwagi, K. Yamaki, M. Tsujimoto, K. Deguchi, N. Orita, T. Koike, R. Nakayama, H. Minami, T. Yamamoto, R. A. Klemm, M. Tachiki, and K. Kadowaki, Geometrical full-wavelength resonance mode generating terahertz waves from a single-crystalline Bi₂Sr₂CaCu₂O_{8+ δ} rectangular mesa, *J. Phys. Soc. Jpn.* **80**, 094709 (2011).
- [26] M. Tsujimoto, I. Kakeya, T. Kashiwagi, H. Minami, and K. Kadowaki, Cavity mode identification for coherent terahertz emission from high- T_c superconductors, *Opt. Express* **24**, 4591 (2016).
- [27] T. Kashiwagi, T. Yuasa, Y. Tanabe, T. Imai, G. Kuwano, R. Ota, K. Nakamura, Y. Ono, Y. Kaneko, M. Tsujimoto, H. Minami, T. Yamamoto, R. A. Klemm, and K. Kadowaki,

- Improved excitation mode selectivity of high- T_c superconducting terahertz emitters, *J. Appl. Phys.* **124**, 033901 (2018).
- [28] H. Zhang, R. Wieland, W. Chen, O. Kizilaslan, S. Ishida, C. Han, W. Tian, Z. Xu, Z. Qi, T. Qing *et al.*, Resonant Cavity Modes in $\text{Bi}_2\text{Sr}_2\text{CaCu}_2\text{O}_{8+x}$ Intrinsic Josephson Junction Stacks, *Phys. Rev. Appl.* **11**, 044004 (2019).
- [29] D. J. Watts and S. H. Strogatz, Collective dynamics of “small-world” networks, *Nature* **393**, 440 (1998).
- [30] L. Ozyuzer, Y. Simsek, H. Koseoglu, F. Turkoglu, C. Kurter, U. Welp, A. E. Koshelev, K. E. Gray, W. K. Kwok, T. Yamamoto, K. Kadowaki, Y. Koval, H. B. Wang, and P. Müller, Terahertz wave emission from intrinsic Josephson junctions in high- T_c superconductors, *Supercond. Sci. Technol.* **22**, 114009 (2009).
- [31] K. Gray, L. Ozyuzer, A. Koshelev, C. Kurter, K. Kadowaki, T. Yamamoto, H. Minami, H. Yamaguchi, M. Tachiki, W.-K. Kwok, and U. Welp, Emission of terahertz waves from stacks of intrinsic Josephson junctions, *IEEE Trans. Appl. Supercond.* **19**, 886 (2009).
- [32] M.-C. Lee and M. Wu, Thermal annealing in hydrogen for 3-D profile transformation on silicon-on-insulator and sidewall roughness reduction, *J. Microelectromech. Syst.* **15**, 338 (2006).
- [33] Jae-Soong Lee, Joonhee Lee, Sunghwan Kim, and Heonsu Jeon, GaN-based light-emitting diode structure with monolithically integrated sidewall deflectors for enhanced surface emission, *IEEE Photonics Technol. Lett.* **18**, 1588 (2006).
- [34] S. P. Zhao, X. B. Zhu, Y. F. Wei, G. H. Chen, Q. S. Yang, and C. T. Lin, $\text{Bi}_2\text{Sr}_2\text{CaCu}_2\text{O}_{8+\delta}$ intrinsic Josephson junctions: Surface layer characterization and control, *Phys. Rev. B* **72**, 184511 (2005).
- [35] H. Eisele, M. Naftaly, and J. R. Fletcher, A simple interferometer for the characterization of sources at terahertz frequencies, *Meas. Sci. Technol.* **18**, 2623 (2007).
- [36] H. Wang, S. Guénon, J. Yuan, A. Iishi, S. Arisawa, T. Hatano, T. Yamashita, D. Koelle, and R. Kleiner, Hot Spots and Waves in $\text{Bi}_2\text{Sr}_2\text{CaCu}_2\text{O}_8$ Intrinsic Josephson Junction Stacks: A Study by Low Temperature Scanning Laser Microscopy, *Phys. Rev. Lett.* **102**, 017006 (2009).
- [37] S. Guénon, M. Grünzweig, B. Gross, J. Yuan, Z. G. Jiang, Y. Y. Zhong, M. Y. Li, A. Iishi, P. H. Wu, T. Hatano, R. G. Mints, E. Goldobin, D. Koelle, H. B. Wang, and R. Kleiner, Interaction of hot spots and terahertz waves in $\text{Bi}_2\text{Sr}_2\text{CaCu}_2\text{O}_8$ intrinsic Josephson junction stacks of various geometry, *Phys. Rev. B* **82**, 214506 (2010).
- [38] A. Yurgens, Temperature distribution in a large $\text{Bi}_2\text{Sr}_2\text{CaCu}_2\text{O}_{8+\delta}$ mesa, *Phys. Rev. B* **83**, 184501 (2011).
- [39] I. Kakeya, Y. Omukai, T. Yamamoto, K. Kadowaki, and M. Suzuki, Effect of thermal inhomogeneity for terahertz radiation from intrinsic Josephson junction stacks of $\text{Bi}_2\text{Sr}_2\text{CaCu}_2\text{O}_{8+\delta}$, *Appl. Phys. Lett.* **100**, 242603 (2012).
- [40] B. Gross, S. Guénon, J. Yuan, M. Y. Li, J. Li, A. Ishii, R. G. Mints, T. Hatano, P. H. Wu, D. Koelle, H. B. Wang, and R. Kleiner, Hot-spot formation in stacks of intrinsic Josephson junctions in $\text{Bi}_2\text{Sr}_2\text{CaCu}_2\text{O}_8$, *Phys. Rev. B* **86**, 094524 (2012).
- [41] T. M. Benseman, A. E. Koshelev, W.-K. Kwok, U. Welp, V. K. Vlasko-Vlasov, K. Kadowaki, H. Minami, and C. Watanabe, Direct imaging of hot spots in $\text{Bi}_2\text{Sr}_2\text{CaCu}_2\text{O}_{8+\delta}$ mesa terahertz sources, *J. Appl. Phys.* **113**, 133902 (2013).
- [42] T. M. Benseman, A. E. Koshelev, W.-K. Kwok, U. Welp, K. Kadowaki, J. R. Cooper, and G. Balakrishnan, The ac Josephson relation and inhomogeneous temperature distributions in large $\text{Bi}_2\text{Sr}_2\text{CaCu}_2\text{O}_{8+\delta}$ mesas for THz emission, *Supercond. Sci. Technol.* **26**, 085016 (2013).
- [43] B. Gross, J. Yuan, D. Y. An, M. Y. Li, N. Kinev, X. J. Zhou, M. Ji, Y. Huang, T. Hatano, R. G. Mints, V. P. Koshelets, P. H. Wu, H. B. Wang, D. Koelle, and R. Kleiner, Modeling the linewidth dependence of coherent terahertz emission from intrinsic Josephson junction stacks in the hot-spot regime, *Phys. Rev. B* **88**, 014524 (2013).
- [44] H. Minami, C. Watanabe, K. Sato, S. Sekimoto, T. Yamamoto, T. Kashiwagi, R. A. Klemm, and K. Kadowaki, Local SiC photoluminescence evidence of hot spot formation and sub-THz coherent emission from a rectangular $\text{Bi}_2\text{Sr}_2\text{CaCu}_2\text{O}_{8+\delta}$ mesa, *Phys. Rev. B* **89**, 054503 (2014).
- [45] C. Watanabe, H. Minami, T. Yamamoto, T. Kashiwagi, R. A. Klemm, and K. Kadowaki, Spectral investigation of hot spot and cavity resonance effects on the terahertz radiation from high- T_c superconducting $\text{Bi}_2\text{Sr}_2\text{CaCu}_2\text{O}_{8+\delta}$ mesas, *J. Phys. Condens. Matter: Inst. Phys. J.* **26**, 172201 (2014).
- [46] M. Ji, J. Yuan, B. Gross, F. Rudau, D. Y. An, M. Y. Li, X. J. Zhou, Y. Huang, H. C. Sun, Q. Zhu *et al.*, $\text{Bi}_2\text{Sr}_2\text{CaCu}_2\text{O}_8$ intrinsic Josephson junction stacks with improved cooling: Coherent emission above 1 THz, *Appl. Phys. Lett.* **105**, 122602 (2014).
- [47] M. Tsujimoto, H. Kambara, Y. Maeda, Y. Yoshioka, Y. Nakagawa, and I. Kakeya, Dynamic Control of Temperature Distributions in Stacks of Intrinsic Josephson Junctions in $\text{Bi}_2\text{Sr}_2\text{CaCu}_2\text{O}_{8+\delta}$ for Intense Terahertz Radiation, *Phys. Rev. Appl.* **2**, 044016 (2014).
- [48] C. Watanabe, H. Minami, T. Kitamura, K. Asanuma, K. Nakade, T. Yasui, Y. Saiwai, Y. Shibano, T. Yamamoto, T. Kashiwagi, R. A. Klemm, and K. Kadowaki, Influence of the local heating position on the terahertz emission power from high- T_c superconducting $\text{Bi}_2\text{Sr}_2\text{CaCu}_2\text{O}_{8+\delta}$ mesas, *Appl. Phys. Lett.* **106**, 042603 (2015).
- [49] X. J. Zhou, J. Yuan, H. Wu, Z. S. Gao, M. Ji, D. Y. An, Y. Huang, F. Rudau, R. Wieland, B. Gross, N. Kinev, J. Li, A. Ishii, T. Hatano, V. P. Koshelets, D. Koelle, R. Kleiner, H. B. Wang, and P. H. Wu, Tuning the Terahertz Emission Power of an Intrinsic Josephson-Junction Stack with a Focused Laser Beam, *Phys. Rev. Appl.* **3**, 044012 (2015).
- [50] T. M. Benseman, A. E. Koshelev, V. Vlasko-Vlasov, Y. Hao, W.-K. Kwok, U. Welp, C. Keiser, B. Gross, M. Lange, D. Kölle, R. Kleiner, H. Minami, C. Watanabe, and K. Kadowaki, Current Filamentation in Large $\text{Bi}_2\text{Sr}_2\text{CaCu}_2\text{O}_{8+\delta}$ Mesa Devices Observed via Luminescent and Scanning Laser Thermal Microscopy, *Phys. Rev. Appl.* **3**, 044017 (2015).
- [51] F. Rudau, R. Wieland, J. Langer, X. J. Zhou, M. Ji, N. Kinev, L. Y. Hao, Y. Huang, J. Li, P. H. Wu, T. Hatano, V. P. Koshelets, H. B. Wang, D. Koelle, and R. Kleiner,

- Three-Dimensional Simulations of the Electrothermal and Terahertz Emission Properties of $\text{Bi}_2\text{Sr}_2\text{CaCu}_2\text{O}_8$ Intrinsic Josephson Junction Stacks, *Phys. Rev. Appl.* **5**, 044017 (2016).
- [52] M. Tsujimoto, T. Doi, G. Kuwano, A. Elarabi, and I. Kakeya, Engineering and characterization of a packaged high- T_c superconducting terahertz source module, *Supercond. Sci. Technol.* **30**, 064001 (2017).
- [53] See Supplemental Material at <http://link.aps.org/supplemental/10.1103/PhysRevApplied.13.014035> for supplemental experiment data.
- [54] T. Kashiwagi, T. Yamamoto, H. Minami, M. Tsujimoto, R. Yoshizaki, K. Delfanazari, T. Kitamura, C. Watanabe, K. Nakade, T. Yasui *et al.*, Efficient Fabrication of Intrinsic-Josephson-Junction Terahertz Oscillators with Greatly Reduced Self-Heating Effects, *Phys. Rev. Appl.* **4**, 054018 (2015).
- [55] I. Kakeya, N. Hirayama, Y. Omukai, and M. Suzuki, Temperature dependence of terahertz emission by an asymmetric intrinsic Josephson junction device, *J. Appl. Phys.* **117**, 043914 (2015).
- [56] L. Y. Hao, M. Ji, J. Yuan, D. Y. An, M. Y. Li, X. J. Zhou, Y. Huang, H. C. Sun, Q. Zhu, F. Rudau *et al.*, Compact Superconducting Terahertz Source Operating in Liquid Nitrogen, *Phys. Rev. Appl.* **3**, 024006 (2015).
- [57] T. Kashiwagi, M. Tsujimoto, T. Yamamoto, H. Minami, K. Yamaki, K. Delfanazari, K. Deguchi, N. Orita, T. Koike, R. Nakayama *et al.*, High temperature superconductor terahertz emitters: Fundamental physics and its applications, *Jpn. J. Appl. Phys.* **51**, 010113 (2011).
- [58] L. N. Bulaevskii and A. E. Koshelev, Radiation due to Josephson Oscillations in Layered Superconductors, *Phys. Rev. Lett.* **99**, 057002 (2007).
- [59] S. Lin and X. Hu, Possible Dynamic States in Inductively Coupled Intrinsic Josephson Junctions of Layered High- T_c Superconductors, *Phys. Rev. Lett.* **100**, 247006 (2008).
- [60] A. E. Koshelev, Alternating dynamic state self-generated by internal resonance in stacks of intrinsic Josephson junctions, *Phys. Rev. B* **78**, 174509 (2008).
- [61] A. E. Koshelev and L. N. Bulaevskii, Resonant electromagnetic emission from intrinsic Josephson-junction stacks with laterally modulated Josephson critical current, *Phys. Rev. B* **77**, 014530 (2008).
- [62] A. E. Koshelev, Stability of dynamic coherent states in intrinsic Josephson-junction stacks near internal cavity resonance, *Phys. Rev. B* **82**, 174512 (2010).